

Supplementary

Behavioral and Sensory Deficits Associated with Dysfunction of GABAergic System in a novel *shank2*-Deficient Zebrafish Model

Yi Wang ¹, Chunxue Liu ¹, Jingxin Deng ¹, Qiong Xu ¹, Jia Lin ², Huiping Li ¹, Meixin Hu ¹, Chunchun Hu ¹, Qiang Li ² and Xiu Xu ^{1,*}

¹ Division of Child Health Care, Children's Hospital of Fudan University, National Children's Medical Center, 399 Wanyuan Road, Shanghai 201102, China

² Center for Translational Medicine, Institute of Pediatrics, Shanghai key Laboratory of Birth Defect, Children's Hospital of Fudan University, National Children's Medical Center, 399 Wangyuan Road, Shanghai 201102, China

* Correspondence: Xiu Xu: xuxiu@shmu.edu.cn

Supplementary Table S1: gRNA gene-target sequences, primers for PCR genotyping and RT-qPCR used in this study.

Supplementary Table S2: Protein homology analysis of zebrafish *shank2a*, *shank2b* and human SHANK2.

Supplementary Table S3: Domains homology analysis of zebrafish *shank2a* and human SHANK2.

Supplementary Table S4: Domains homology analysis of zebrafish *shank2b* and human SHANK2.

Supplementary Table S5: Homology comparison between zebrafish *shank2a* and *shank2b*

Supplementary Table S6: Phenotypic characteristics of zebrafish embryos at 24 hpf.

Supplementary Table S7: Phenotypic characteristics of zebrafish embryos at 3 dpf.

Supplementary Figure S1: *shank2* orthologues are conserved in zebrafish and CRISPR-Cas9 induced *shank2b* target-mutation

Supplementary Figure S2: Morphological analysis of *shank2b*^{-/-} zebrafish

Supplementary Figure S3: *shank2b* mutants exhibited normal VMR response to darkness stimuli

Supplementary Figure S4: Dose-response paired plots showing the change in activity during light to dark transition per fish of wild-type or *shank2b*^{-/-} fish at 9dpf exposed to water or increasing concentrations of Pentylene-tetrazol (PTZ) for 1 h

Supplementary Figure S5: Different isoforms of zebrafish *shank2a*

Supplementary Figure S6: Different isoforms of zebrafish *shank2b*

Supplementary Table S1. gRNA gene-target sequences, primers for PCR genotyping and RT-qPCR used in this study

Primer	Sequence (5'-3')	Gene ID
<i>shank2b</i> -gRNA target site-E10	GGATCGGAGCAGCACTCGCG	NC_07136.7
<i>shank2b</i> -genotyping PCR-Intron9-F	TGTATGCAGAAATGAAGCTGAAGT GTG	NC_07136.7
<i>shank2b</i> -genotyping PCR-E10/I10-R	AATGTGGGAAGATCACTGACCTGC	
<i>shank2b</i> -qPCR-E10-F	GCCCCGCGAGTGCTGCTC	NM_00112834
<i>shank2b</i> -qPCR-E10-R	CCATGGTTTTACCGTGCCA	7.1
<i>shank2a</i> -qPCR-E2/3-F	ATCGGATCAAGAGAATGGATGGCT	ENSDART000
<i>shank2a</i> -qPCR-E3-R	TGAAACACTGCTCTGCGTTCCC	00159950.2
<i>gabra1</i> -qPCR-F	GGAGAGCGTGTAACCGAAGTCAA G	NM_00107732
<i>gabra1</i> -qPCR-R	TTGTTGAGACGGAGCACGGC	6.1
<i>gabara2a</i> -qPCR-F	TTCTCACGGATTTCTAATCCACCTG	XM_009307207
<i>gabara2a</i> -qPCR-R	TCTGTCACTCGATCTCCAAGACCA	.3
<i>gabara3</i> -qPCR-F	TGAAGTTCGGGAGCTATGCCTACA	XM_021469255
<i>gabara3</i> -qPCR-R	TGGTCTCTTTGCCGATGACGTG	.1
<i>gabara4</i> -qPCR-F	TGTCTTTGGAATCACCACCGTCC	NM_00101782
<i>gabara4</i> -qPCR-R	GCGTTGGTAAAGTAGTTGACGGCC	2.1
<i>gabara5</i> -qPCR-F	TTTGACCTGCCATCTGAGCCTCT	XM_005166083
<i>gabara5</i> -qPCR-R	TGGTCAAAGCTGGTAACAAAGA TG	.4
<i>gabara6a</i> -qPCR-F	TTGGAAGCTATGCTTACACGAATC G	NM_200731.1
<i>gabara6a</i> -qPCR-R	TGGACGACCTGGACAGAATACAG TC	
<i>gabara6b</i> -qPCR-F	TGACCACTCCAACAAGCTGTTC	XM_002667357
<i>gabara6b</i> -qPCR-R	TCACCTGTGTTGACTTCAACCTTT C	.6
<i>gabrb1</i> -qPCR-F	CTCAGGATAACGACTACCGCTGCA	XM_021480764
<i>gabrb1</i> -qPCR-R	CGGCAGCTCGATGTTGTCCA	.1
<i>gabrb2a</i> -qPCR-F	ATTAAGGATCACCACCACCGCTG	NM_00102438
<i>gabrb2a</i> -qPCR-R	GCAGTTCGATTCTCTCCACCCC	7.2
<i>gabrb3</i> -qPCR-F	TGACACAAGCGCCAATGAACC	XM_021471811
<i>gabrb3</i> -qPCR-R	ACCTCAGACACCATGTCTATGCTC G	.1
<i>gabrb4</i> -qPCR-F	ACTTTGGAGGTCCTCCAGTCATCG	XM_017353011
<i>gabrb4</i> -qPCR-R	GCCACACGGTTGTCCAAAGTCA	.2
<i>gabrg1</i> -qPCR-F	TCATTAGGCATCACAACCTGTGCTC A	XM_009307208
<i>gabrg1</i> -qPCR-R	GCTTGTGAAATAATGCAGAGTCC	.3

	G	
<i>gabrg2</i> -qPCR-F	CACTTTAAGGTTGACCATTGACGC A	NM_00125625 0.1
<i>gabrg2</i> -qPCR-R	CGGATATCTCCAACCTCCACAGAG C	
<i>gabrd</i> -qPCR-F	TCAGAAGCCAACATGGAATACAC CA	XM_695007.8
<i>gabrd</i> -qPCR-R	TTCTCCACCGTCACGTCATGAAA	
<i>RPL13A(60s)</i> -qPCR-F	TCTGGAGGACTGTAAGAGGTATGC	ENSDART000 00023156
<i>RPL13A(60s)</i> -qPCR-R	AGACGCACAATCTTGAGAGCAG	

Supplementary Table S2. Protein homology analysis of zebrafish shank2a, shank2b and human SHANK2

Gene	NCBI reference mRNA number	NCBI reference protein number	Amino acid	vs. human SHANK2 protein (NP_036441.2)	
				Query cover (%)	Identity (%)
<i>shank2a</i>	XM_021467943.1	XP_021323618.1	1707	100%	46.63%
<i>shank2b</i>	NM_001128347.1	NP_001121819.1	1800	100%	60.58%

Supplementary Table S3. Domains homology analysis of zebrafish shank2a and human SHANK2

shank2a domains	NCBI reference protein number	vs. human SHANK2 protein domains (NP_036441.2)	
		Query cover (%)	Identity (%)
ANK	XP_021323618.1	94%	74.23%
PDZ		100%	82.80%
SAM		100%	75.38%

Supplementary Table S4. Domains homology analysis of zebrafish shank2b and human SHANK2

shank2b domains	NCBI reference protein number	vs. human SHANK2 protein domains (NP_036441.2)	
		Query cover (%)	Identity (%)
ANK	NP_001121819.1	100%	80.50%
SH3		100%	76.92%
PDZ		100%	92.55%
SAM		100%	88.06%

Supplementary Table S5 Homology comparison between zebrafish shank2a and shank2b

	NCBI reference protein number	shank2a vs shank2b	
		Query cover (%)	Identity (%)
shank2a	NP_001121819.1	100%	49%
shank2b	XP_021323618.1	-	-
ANK		85%	71%
SH3		-	-
PDZ		100%	83%

Supplementary Table S6. Phenotypic characteristics of zebrafish embryos at 24 hpf

Genotype	Developmental delay	Death	Normal	Total
<i>shank2b^{+/+}</i> (WT)	1 (1.4%)	19 (26.8%)	51 (71.8%)	71 (100%)
<i>shank2b^{+/-}</i>	0 (0%)	8 (12.5%)	56 (87.5%)	64 (100%)
<i>shank2b^{-/-}</i>	0 (0%)	22 (28.9%)	54 (71.1%)	76 (100%)
Total	1 (0.5%)	49 (23.2%)	161 (76.3%)	211 (100%)

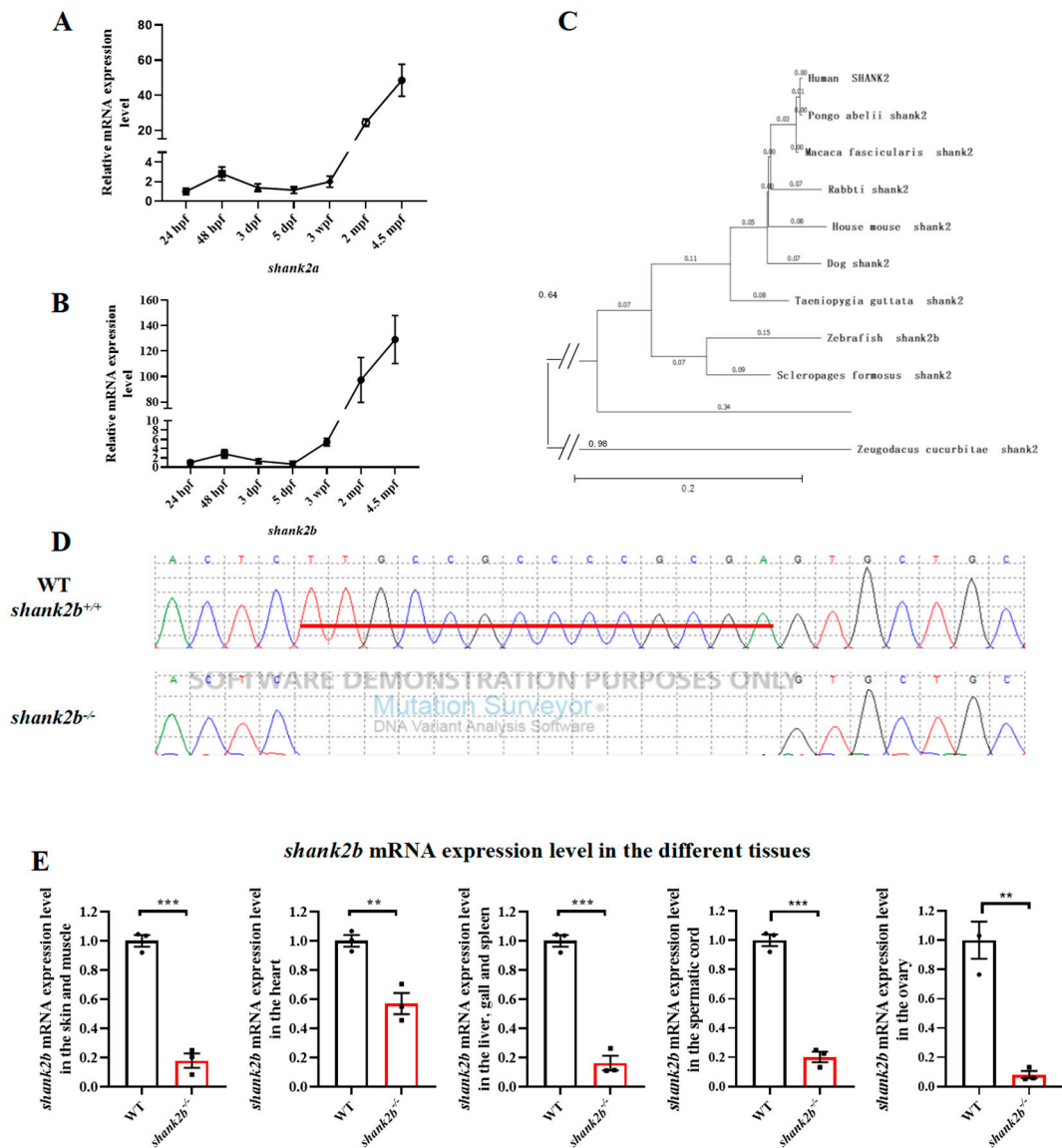
Supplementary Table S5: Person Chi-squared Test, P = 0.088.

Supplementary Table S7. Phenotypic characteristics of zebrafish embryos at 3 dpf

Genotype	Developmental delay	Death	Normal	Total
<i>shank2b^{+/+}</i> (WT)	1 (1.4%)	19 (26.8%)	51 (71.8%)	71 (100%)
<i>shank2b^{+/-}</i>	0 (0%)	8 (12.5%)	56 (87.5%)	64 (100%)
<i>shank2b^{-/-}</i>	0 (0%)	22 (28.9%)	54 (71.1%)	76 (100%)
Total	1 (0.5%)	49 (23.2%)	161 (76.3%)	211 (100%)

Supplementary Table S6: Person Chi-squared Test, P = 0.088.

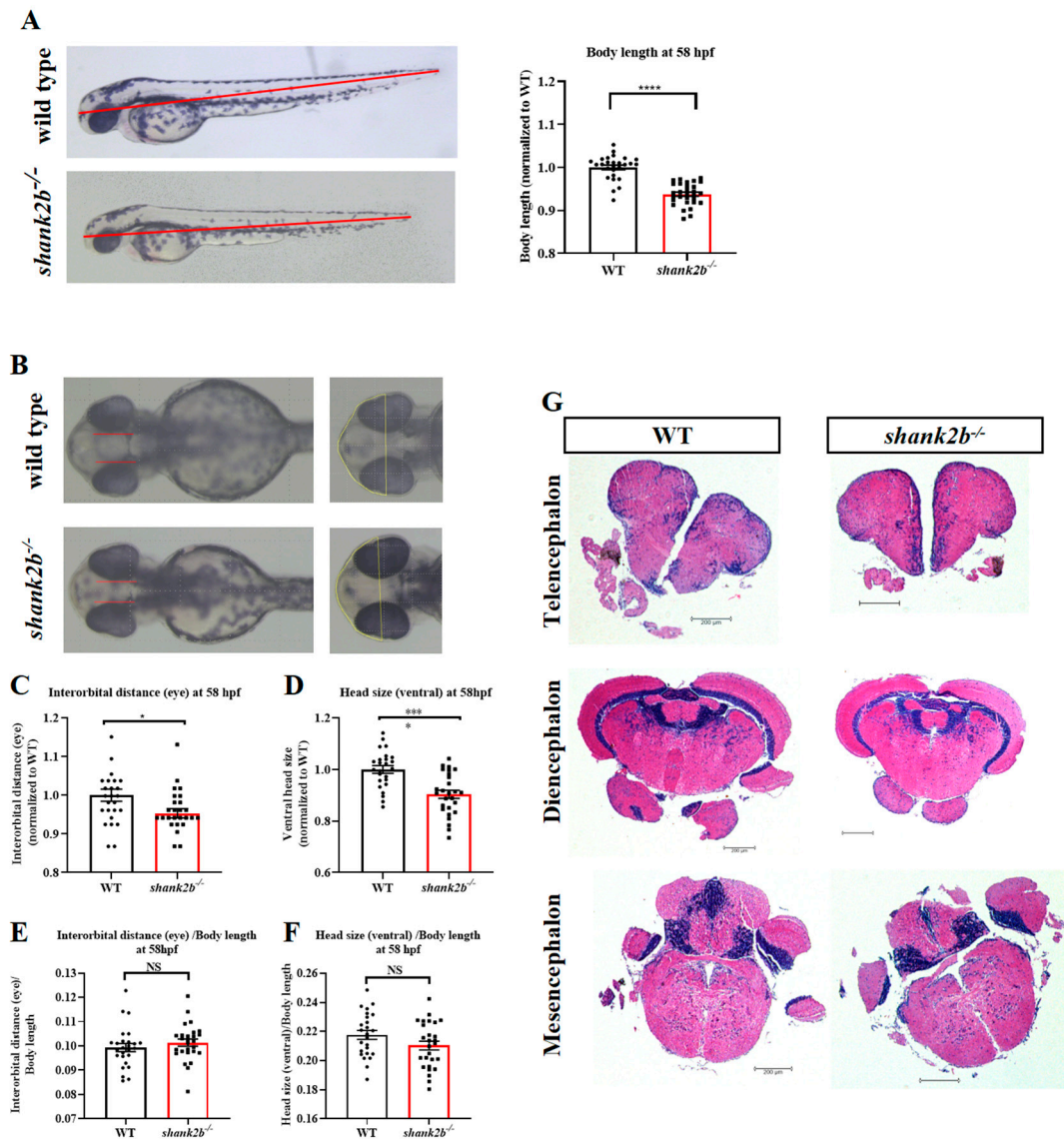
Supplementary Figure S1



Supplementary Figure S1 *shank2* orthologues are conserved in zebrafish and CRISPR-Cas9 induced *shank2b* target mutation. **A-B** Temporal mRNA expression profiling of zebrafish *shank2a* and *shank2b* at seven stages: 24 hpf, 48 hpf, 3 dpf, 5 dpf, 3 wpf, 2 mpf and 4.5 mpf. Data are shown as mean \pm SEM, $n = 3-4$. **C** Phylogenetic analysis of SHANK2 in 10 species. The phylogenetic tree was constructed using the neighbor-joining methods as implemented in the MEGA 6 package. All of the sequences are available from the NCBI protein database. *Human*, NP_036441.21, *Pongo abelii*, XP_024111518, *Macaca fascicularis*, XP_015290734.1, *Rabbit*, XP_002723176, *House mouse*, NP_001074839.3, *Dog*, XP_022260831, *Taeniopygia guttata*, XP_030129375, *Scleropages formosus*, XP_029112011.1, *Zeugodacus cucurbitae*, XP_028896935.1, *Danio rerio shank2a*, XP_021323618.1, *Danio rerio shank2b*, NP_001121819.1. The obtained numbers represented evolutionary relationships, with larger numbers indicating greater genetic differences. In vertebrate animals, the genetic distance was not greater than "0.35". In invertebrates (such as *Zeugodacus cucurbitae*), the distance was as high as "0.98". **D** Sanger sequence confirmation of 14-nucleotide deletion mutations highlighted in red. **E** Reduced

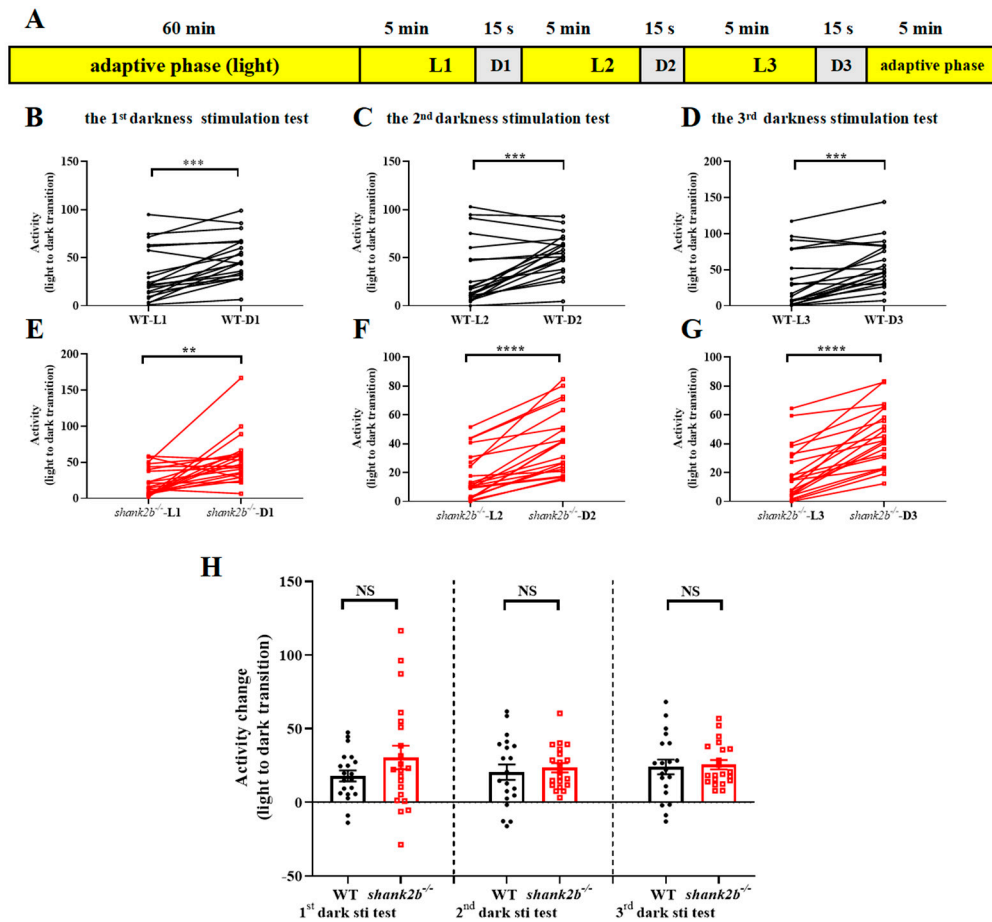
expression of *shank2b* mRNA in the other tissues of 4.5 mpf male *shank2b*^{-/-} mutants (Skin and muscle, ****p* = 0.0002; Heart, ***p* = 0.0065; Liver, Gall and Spleen, ****p* = 0.0002). Reduced expression of *shank2b* mRNA in the ovary of female *shank2b*^{-/-} (** *p* = 0.0021) and spermatic cord of male mutants at 4.5 mpf (****p* = 0.0001). Each group n = 3. Student's t test. Data are shown as mean ± SEM.

Supplementary Figure S2



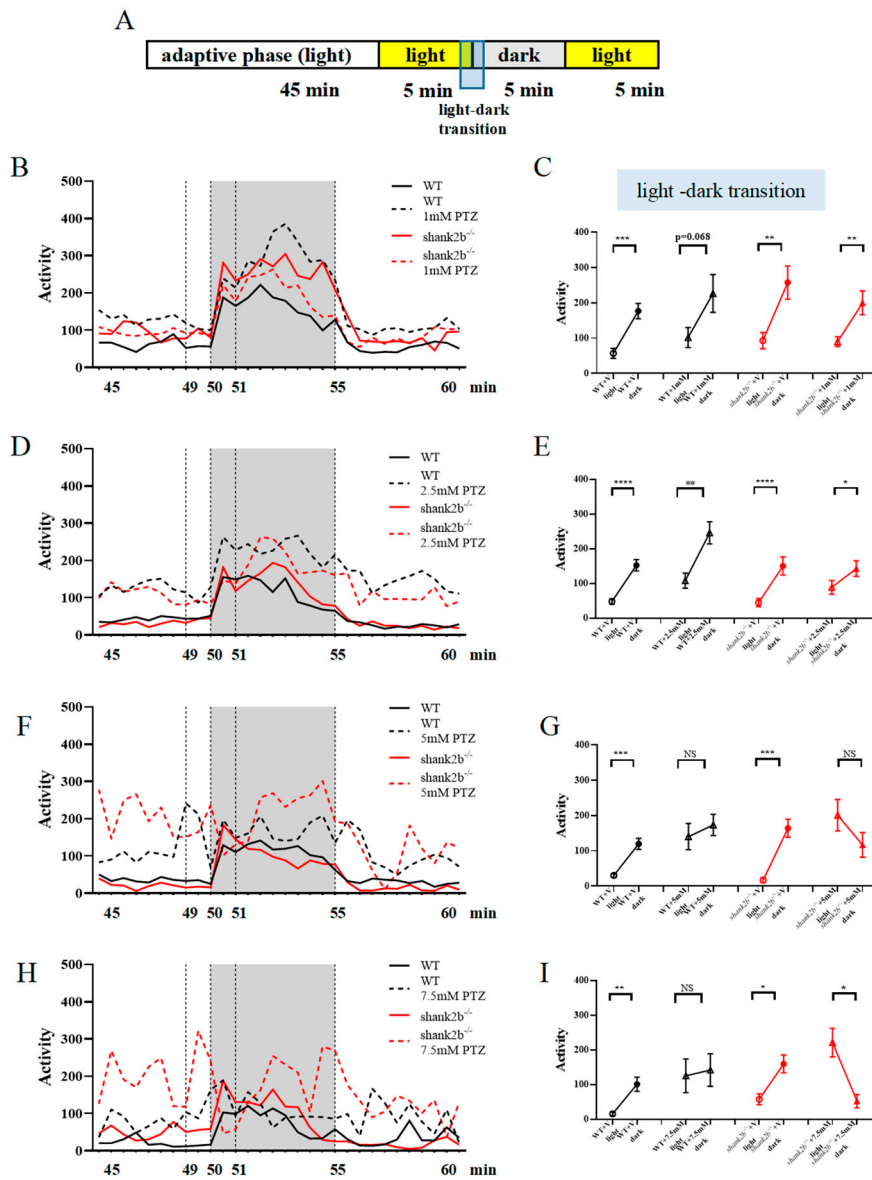
Supplementary Figure S2 Morphological analysis of *shank2b*^{-/-} zebrafish. **A** The body length of *shank2b* mutants at 58 hpf were shorter in body length than WT larvae (WT n = 27, *shank2b*^{-/-} n = 30, **** $p < 0.0001$, Student's t test). Data are presented as mean \pm SEM. **B-F** Head size in wild-type and *shank2b* mutant were measured from dorsal and ventral images using Image J. Representative tracings, the distance between the convex tips of the eyes, done in Image J are shown in red, as well as the boundaries of forebrain-midbrain in yellow. The head size appears to be smaller in mutants (**B, C, D**) larvae at 58 hpf eye interorbital distance, WT n = 26, *shank2b*^{-/-} n = 27, * $p = 0.0222$, Student's t test; ventral head size, WT n = 25, *shank2b*^{-/-} n = 27, **** $p < 0.0001$, Student's t test). (**E, F**) The ratio of Interorbital distance (eye)/ body length (WT n = 26, *shank2b*^{-/-} n = 27, ns, $p = 0.3688$) and Head size (ventral)/ body length (WT n = 25, *shank2b*^{-/-} n = 27, ns, $p = 0.0947$, Student's t test) at 58 hpf between WT and mutants showed no significant difference. Data are presented as mean \pm SEM. **G** Examination of brain tissues in WT (left images) and *shank2b*^{-/-} (right images) by H&E staining at 4.5 mpf. Zebrafish brains were sectioned at telencephalic, diencephalic and mesencephalic levels. Scale bar = 200 μ m.

Supplementary Figure S3



Supplementary Figure S3 *shank2b* mutants exhibited normal VMR response to darkness stimuli. **A** Scheme and behavioral setup applied for locomotor activity tracking in VMR response to darkness stimulation of zebrafish larvae at 13 dpf. The experiment consisted of one 60-min adaptation period under continuous illumination and one 20-min 45-s testing period consisting of three VMR tests. One VMR experiment consisted of 5 min of conditioning to illumination and 15 s of stimulation by a sudden darkness stimuli. **B-G (E-G)** *shank2b*^{-/-} models exhibited normal response (first dark stimuli, ** $p = 0.001$; second dark stimuli, **** $p < 0.0001$; third dark stimuli, **** $p < 0.0001$, $n = 21$, Paired t test), characterized by dramatic increases in movement in response to three sudden transitions from light to darkness, similar to WT larvae (**B-D**) (first dark stimuli, **** $p < 0.0001$; second dark stimuli, *** $p = 0.0009$; third dark stimuli, *** $p = 0.001$; $n = 20$, Paired t test). (**H**) Column plots compare activity detected during the 1 min before and the 15 s after each darkness stimulation exposure between WT and *shank2b* mutants. Both WT and *shank2b* larva were sensitive to dark stimuli, manifested as no significant difference in activity change three times from light to dark (first dark stimuli, ns $p = 0.1667$; second dark stimuli, ns $p = 0.6332$; third dark stimuli, ns $p = 0.7971$; WT $n = 20$, *shank2b*^{-/-} $n = 21$, Student's t test). Data are presented as the mean \pm SEM.

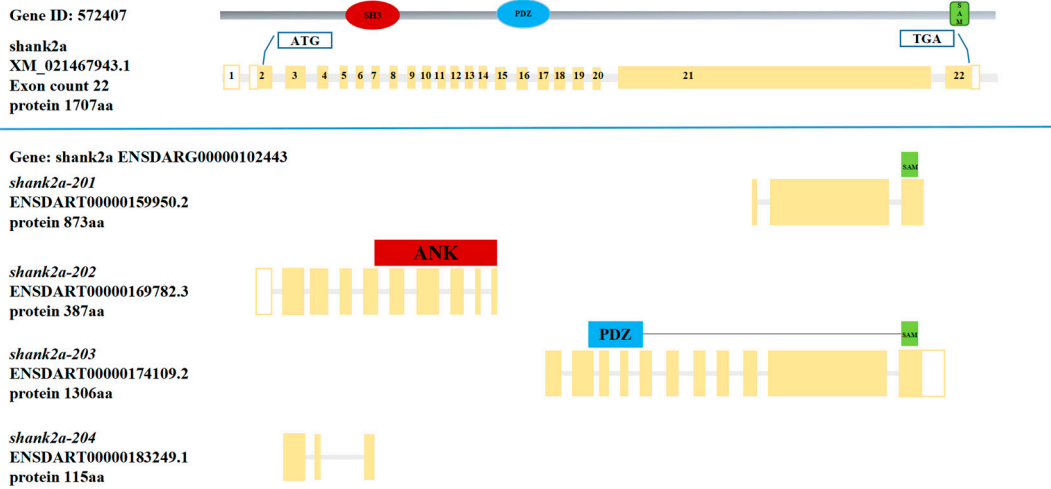
Supplementary Figure S4



Supplementary Figure S4 Dose-response paired plots showing the change in activity during light to dark transition per fish of wild-type or *shank2b*^{-/-} fish at 9dpf exposed to water or increasing concentrations of pentylenetetrazol (PTZ) for 1 h. A PTZ dose-response behavioral experimental procedure. The experiment consisted of a 45-min adaptation period of light condition and a 15-min testing period consisting of one light-dark cycle, consisted of 5 min of conditioning to light and 5 min of darkness stimulation. **B-I Experiments were performed at 9 dpf. (**B, D, F, H**) The horizontal axis denotes the experimental progression of the testing period. The vertical axis denotes the activity detected by larvae in each 30-seconds time bin. PTZ concentration information is marked on the top right corner of each panel. Data are presented as the mean. (**C, E, G, I**) Effects of PTZ treatment on locomotor activity during light-dark transitions. Paired dot plots compared average swimming distances per larva of the light conversions in the one min before and after the light-to-dark conversions. Data are presented as the mean ± SEM. (**C**) PTZ concentrations of 1 mM of WT and *shank2b*^{-/-} fish exhibited an**

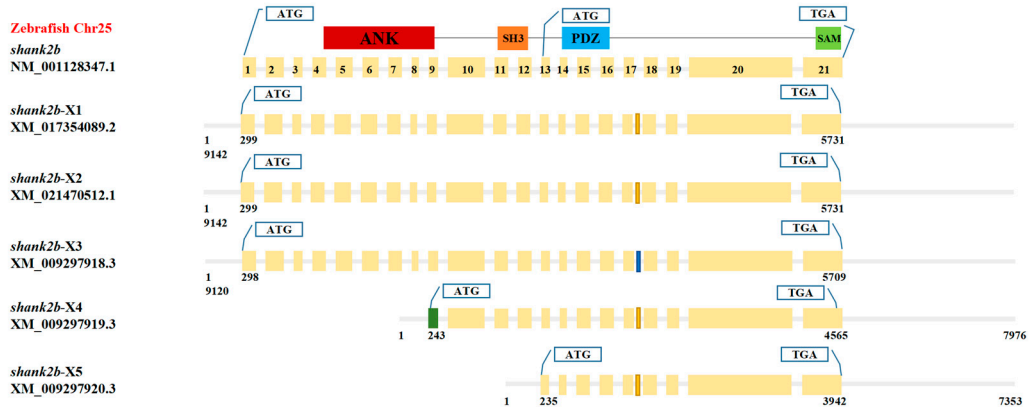
dynamic increase of activity during light-dark transitions, which means that no change had been induced compared with untreated larvae at 9 dpf (WT n = 12, *** $p = 0.0002$; WT + 1 mM n = 11, ns, $p = 0.0668$; *shank2b^{-/-}* n = 10, ** $p = 0.0052$; *shank2b^{-/-}* + 1 mM n=12, ** $p = 0.0062$; Paired t test). (E) PTZ concentrations of 2.5 mM of WT and *shank2b^{-/-}* fish didn't elicit a decline in activity (WT n = 18, **** $p < 0.0001$; WT + 2.5 mM n = 18, ** $p = 0.0022$; *shank2b^{-/-}* n = 18, **** $p < 0.0001$; *shank2b^{-/-}* + 2.5 mM n=18, * $p = 0.0459$; Paired t test). (G) The activity of PTZ-treated WT larvae also increased at concentrations of 5 mM, whereas 5 mM PTZ-treated *shank2b^{-/-}* slightly decreased. Although these results did not achieve statistical significance (WT n = 16, *** $p = 0.0001$; WT + 5 mM n = 15, ns, $p = 0.4365$; *shank2b^{-/-}* n = 12, *** $p = 0.0001$; *shank2b^{-/-}* + 5 mM n=12, ns, $p = 0.1393$; Paired t test). (I) 7.5 mM PTZ-treated *shank2b^{-/-}* significantly decreased during the light-dark transition, whereas 7.5 mM PTZ-treated WT larvae also increased without statistical significance (WT n = 6, ** $p = 0.0039$; WT + 7.5 mM n = 6, ns, $p = 0.7292$; *shank2b^{-/-}* n = 6, * $p = 0.0136$; *shank2b^{-/-}* + 7.5 mM n=6, * $p = 0.0292$; Paired t test).

Supplementary Figure S5



Supplementary Figure S5 Different isoforms of zebrafish *shank2a*. Sequence data from NCBI and Ensembl

Supplementary Figure S6



Supplementary Figure S6 Different isoforms of zebrafish *shank2b*. Sequence data from NCBI